CANCER GENOMICS & PROTEOMICS *17*: 781-793 (2020)
doi:10.21873/cgp.20232

Gigantol Targets MYC for Ubiquitin-proteasomal Degradation and Suppresses Lung Cancer Cell Growth

NATTANAN LOSUWANNARAK[1,2], SITTIRUK ROYTRAKUL[3] and PITHI CHANVORACHOTE[1,2]

[1]Cell-Based Drug and Health Product Development Research Unit, Faculty of Pharmaceutical Sciences, Chulalongkorn University, Bangkok, Thailand;
[2]Department of Pharmacology and Physiology, Faculty of Pharmaceutical Sciences, Chulalongkorn University, Bangkok, Thailand;
[3]Functional Ingredients and Food Innovation Research Group, National Center for Genetic Engineering and Biotechnology, National Science and Technology Development Agency, Pathumthani, Thailand

Abstract. *Background: Gigantol is a pharmacologically active bibenzyl compound exerting potential anticancer activities. At non-toxic concentrations, it reduces cancer stem cell properties and tumorigenicity. The mechanisms of the effects of gigantol on cancer cell growth are largely unknown. This study aimed to unravel the molecular profile and identify the prominent molecular mechanism of the effects of gigantol in controlling lung cancer cell proliferation. Materials and Methods: Proteomics and bioinformatics analysis were used accompanied by experimental molecular pharmacology approaches. Results: Gigantol exhibited antiproliferative effects on human lung cancer cells confirmed by 3-(4, 5-dimethylthiazol-2-yl)-2, 5-diphenyltetrazolium bromide proliferation assay and colony growth assay. The protein profile in response to gigantol treatment associated with regulation of cell proliferation was analyzed to determine the prominent protein targets. Among the significant hub proteins, MYC, an important proto-oncogene and proliferation-promoting transcription factor, was down-regulated with the highest number of protein–protein interactions. MYC down-regulation was confirmed by western blot analysis. The up-stream regulator of MYC, Glycogen synthase kinase 3 beta (GSK3β) was found to be responsible for MYC destabilization mediated by gigantol. Gigantol facilitated GSK3β function and resulted in the increase of MYC–ubiquitin complex as evaluated by immunoprecipitation. Conclusion: Gigantol was found to inhibit lung cancer proliferation through induction of GSK3β-mediated MYC ubiquitin-proteasome degradation. These data suggest gigantol to be a promising candidate for novel strategy in inhibition of lung cancer.*

Evading growth suppression and sustaining proliferation are among the hallmarks of cancer and lead to disease progression (1). Cell proliferation is an increase in the number of cells as a result of cell growth and cell division, and rapid proliferation is considered an aggressive factor of cancer and is correlated with poor prognosis (2, 3). Dysregulation of proliferation signals and oncogenes is known to drive carcinogenesis and tumor growth (4, 5).

There are several oncogenes that control cancer cell growth. MYC, a proto-oncogene, is a central transcription factor that controls cell proliferation, differentiation, and apoptosis. Amplification or overexpression of *MYC* occurs in various cancer types, including lung cancer, and was shown to be related to poor survival (6). An inhibition of MYC may offer an effective therapeutic treatment *via* tumor growth suppression (7, 8). However, as targeted therapy against MYC is still elusive due to its lack of inhibitory binding site, modulation of the MYC level *via* targeting its up-stream regulators is a potential strategy (6). Glycogen synthase kinase 3 beta (GSK3β) showed prominent tumor-suppressor properties in lung cancer (9). Protein kinase B (AKT1)-dependent GSK3β phosphorylation at Ser9 was shown to be correlated with poor survival rate of patients with lung cancer (10). GSK3β suppresses cancer cell proliferation by inhibit various oncoproteins, including MYC. The active GSK3β mediates degradation of MYC *via* phosphorylation at Thr58 (11). Indirect attenuation of MYC stabilization may offer an effective therapeutic treatment *via* tumor growth suppression.

Correspondence to: Professor Dr. Pithi Chanvorachote, Department of Pharmacology and Physiology, Faculty of Pharmaceutical Sciences, Chulalongkorn University, 254 Phayathai Road, Pathumwan, Bangkok 10330, Thailand. Tel: +662 2188344, Fax: +662 2188324, e-mail: pithi_chan@yahoo.com

Key Words: Gigantol, Dendrobium draconis, MYC, proteomics, cell proliferation, lung cancer.

Gigantol is a bibenzyl compound from orchids, such as *Dendrobium draconis* (Figure 1). Gigantol was shown to have anticancer activity by triggering apoptotic cell death *via* a caspase-dependent mechanism at high concentrations (12). In addition, non-toxic concentrations of gigantol led to epithelial-to-mesenchymal transition (EMT inhibition) and suppression of migration and invasion (13), and reduction of cancer stem cell-like phenotype (14). Nevertheless, the basis for tumor growth suppression by gigantol is largely unknown. Proteomic analysis is a systematic mean for identification and quantification of the complete protein profile. This approach benefits the investigation of molecular pharmacology by allowing monitoring of proteins affected in response to a drug or active compound leading to the identification of major drug mechanism. This study aims at evaluated the effect of gigantol on lung cancer cell proliferation and defined the major molecular mechanisms of action. These data may benefit the development of gigantol for novel cancer treatment as well as provide the overall information of cellular proteins affected by this compound.

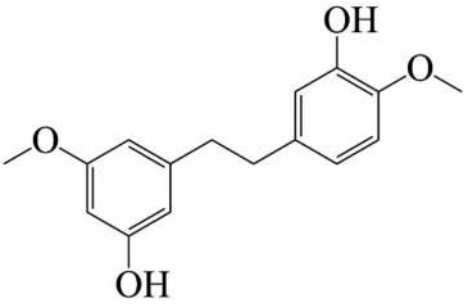

Figure 1. *Gigantol structure*.

Materials and Methods

Cell cultures. H460, A549, and H292 Human lung carcinoma cell lines were purchased from the American Type Culture Collection (Manassas, VA, USA). Lung cancer cells were cultured in Roswell Park Memorial Institute (RPMI)-1640 medium in a humidified atmosphere with 5% CO_2 at 37˚C. The medium was supplemented with 10% fetal bovine serum, 2 mM L-glutamine, and 100 units/ml of each penicillin and streptomycin.

Chemicals and reagents. Gigantol, 3-(4,5-dimethylthiazol-2-yl)-2,5-diphenyltetrazolium bromide (MTT), cycloheximide, MG132, bovine serum album, dimethyl sulfoxide (DMSO), fetal bovine serum (FBS), and cocktail protease inhibitor mixture were purchased from Sigma Chemical, Inc. (Chemical Express, Bangkok, Thailand). RPMI-1640 medium, phosphate buffer saline, glutamine, penicillin, and streptomycin were purchased from Gibco Company (Gibthai, Bangkok, Thailand). Primary and secondary antibodies for western blot analysis and RIPA buffer were purchased from Cell Signaling Technology, Inc. (Theera Trading, Bangkok, Thailand).

Cell viability test: MTT assay. Cells were seeded at a density of 8×10^3 cells per well in 96-well plates. When the cells had adhered, the medium was removed, and medium with different concentrations of gigantol (0-200 μM) was added. After 24 h of treatment, the number of viable cells was measured by MTT assay. The medium was aspirated, and 0.4 mg/ml of MTT in PBS was added to each well. The plate was incubated at 37˚C with 5% CO_2 for 3 h. Afterward, the resulting formazan crystals were dissolved in 100 μl of DMSO and subjected to absorbance reading at 570 nm *via* a microplate reader (ClarioStar, BMG Labtech, Germany).

Proliferation assay. MTT assay was used to determine the antiproliferative activity of non-toxic concentrations of gigantol. Cells were seeded at a density of 2×10^3 cells per well in 96-well plates. When the cells had adhered, the medium was replaced with 5-20 μM of gigantol or vehicle in complete medium. MTT assay was performed at 0, 24, 48, 72 h after treatment. The growth rate of each treatment group was normalized by its own MTT result at the 0 h time. The growth rates were compared to the untreated group at each time point.

Colony-formation assay. Cells were seeded at a density of 500 cells per well in a 6-well plate. When the cells had adhered, the medium was replaced with 5-20 μM of gigantol or vehicle in complete medium. The medium with or without gigantol was replaced every 3 days. After incubation for 10 days, the cells were fixed and stained with crystal violet staining solution. The cells were photographed, and the colonies with ≥50 cells were counted. The numbers of colonies of gigantol-treated groups were compared to those of the control groups.

Sample preparation for proteomics analysis. H460 cells were treated with 20 μM gigantol or 0.004% DMSO (vehicle) for 24 h. The cells were then lysed with 0.5% sodium dodecyl sulfate. The total protein amount collected from each sample was measured with Lowry assay with bovine serum albumin as a standard. Equal amounts of protein from three independent biological samples was pooled. Fifty micrograms of protein from control or gigantol-treated cells were subjected to in-solution digestion. Samples were completely dissolved in 10 mM ammonium bicarbonate (AMBIC), disulfide bonds were reduced using 5 mM dithiothreitol in 10 mM AMBIC at 60˚C for 1 h, and sulfhydryl groups were alkylated by using 15 mM iodoacetamide in 10 mM AMBIC at room temperature for 45 mins in the dark. For digestion, samples were mixed with 50 ng/μl of sequencing grade trypsin (1:20 ratio); (Promega, Walldorf. Germany) and incubated at 37˚C overnight. Prior to analysis by liquid chromatography-tandem mass spectrometry (LC-MS/MS), the digested samples were dried and protonated with 0.1% formic acid before injection into LC-MS/MS.

LC-MS/MS. LC-MS/MS was utilized to identify and quantify the peptides obtained from the digested lysates. The tryptic peptide samples were prepared for injection into an Ultimate3000 Nano/Capillary LC System (Thermo Scientific, Altrincham, UK) coupled to a Hybrid Quadrupole Q-ToF impact II™ MS detector (Bruker Daltonics, Bangkok, Thailand) equipped with a nano-captive spray ion source. Briefly, peptides were enriched on a μ-Precolumn 300 μm i.d. × 5 mm C18 Pepmap 100, 5 μm, 100 A (Thermo Scientific), separated on a 75 μm I.D. × 15 cm column

packed with Acclaim PepMap RSLC C18, 2 μm, 100Å, nanoViper (Thermo Scientific). Solvent A and B containing 0.1% formic acid in water and 0.1% formic acid in 80% acetonitrile, respectively, were supplied to the analytical column. A gradient of 5-55% solvent B was used to elute the peptides at a constant flow rate of 0.30 μl/minute for 30 min. Electrospray ionization was carried out at 1.6 kV using CaptiveSpray. MS and MS/MS spectra were obtained in the positive-ion mode over the m/z range 150-2200 (Compass 1.9 software; Bruker Daltonics).

Bioinformatics and proteomics data analysis. MaxQuant 1.6.6.0 (Max-Planck Institute for Biochemistry, Martinsried, Germany) was used to quantify the proteins in individual samples using the Andromeda search engine to correlate MS/MS spectra to the Uniprot *Homo sapiens* database (https://www.uniprot.org/). The following parameters were used for data processing: Maximum of two miss cleavages, a mass tolerance of 20 ppm for the main search, trypsin as digesting enzyme, carbamidomethylation of cysteine as a fixed modification, and the oxidation of methionine and acetylation of the protein *N*-terminus as variable modifications. Only peptides with a minimum of seven amino acids, as well as at least one unique peptide, were required for protein identification. Only proteins with at least two peptides, and at least one unique peptide, were considered as being identified and used for further data analysis. Protein organization and biological action were investigated conforming to protein analysis through evolutionary relationships (Panther) protein classification (http://pantherdb.org/). Proteins that were uniquely found in gigantol-treated cells were considered as significantly up-regulated, while proteins that were uniquely found in vehicle-treated cells were considered as significantly down-regulated by gigantol, and these differentially expressed proteins were subjected to bioinformatics analysis. The enriched Gene Ontology (GO) annotations were determined by the gene enrichment analysis software Enrichr (http://amp.pharm.mssm.edu/Enrichr/). The Search Tool for Retrieval of Interacting Genes/Proteins (STRING) software version 11 was used to analyze the common and the forecasted functional interaction networks between identified proteins (https://string-db.org/cgi/input.pl). Cytoscape 3.7.2 was utilized to analyze the significant clusters from protein–protein interaction (PPI) networks (https://cytoscape.org/).

Western blot analysis. Western blot assay was used for determination of protein levels. Lung cancer cells were treated with 0-20 μM of gigantol for 24 h. The cells were lysed with RIPA buffer and cocktail protease inhibitor mixture for 30 min on ice. The protein contents of the cell lysates were evaluated by the bicinchoninic acid assay. Samples with equal amounts of protein (30-50 μg) were run on sodium dodecyl sulfate–polyacrylamide gel electrophoresis and were then transferred onto nitrocellulose membranes (Bio-Rad, Hercules, CA, USA). Transferred membranes were blocked for 1 h in 5% non-fat dry milk in Tris buffer saline with 1% Tween 20 (TBST) and incubated overnight with specific primary antibodies against interested proteins. Membranes were washed three times with TBST and incubated with appropriate horseradish peroxidase (HRP)-labeled secondary antibodies for 2 h at room temperature. The immune complexes were detected by SuperSignal™ West Pico PLUS Chemiluminescent Substrate (Thermo Scientific) or Immobilon Western Chemiluminescent HRP Substrate (Millipore) and were imaged using ImageQuant LAS 4000 biomolecular imager (GE Healthcare, Chicago, IL, USA).

Cycloheximide chasing assay. Cells were treated with 20 μM gigantol with or without 50 μg/ml cycloheximide for 0, 15, 30, 45, 60 and 90 min. The treated cells were collected and lysed with RIPA buffer containing protease inhibitor cocktail. Western blot analysis was performed for detecting the MYC protein level. Protein band intensities were analyzed using ImageJ software (version 1.52; National Institutes of Health, Bethesda, MD, USA), and the MYC protein half-life was calculated.

Immunoprecipitation assay. Cells were pretreated with 10 μM proteasome inhibitor, MG132, for 1 h in order to prevent the ubiquitinated MYC from proteasomal degradation and treated with 20 μM of gigantol or left untreated for 1 h. The cells were collected and lysed with RIPA buffer containing protease inhibitor cocktail. Immunoprecipitation was then performed using Dynabeads™ Protein G Immunoprecipitation Kit from Thermo Fisher Scientific Inc. (Waltham, MA, USA). Magnetic beads were prepared and resuspended with primary antibody against MYC (1:50) in a binding buffer for 10 min. A suspension of the magnetic bead–antibody complex was mixed with cell lysate and incubated at 4˚C overnight to allow MYC antigen to bind with magnetic bead–antibody complex. After that, the magnetic bead–antibody–antigen complex was washed three times using 200 μl of washing buffer, separated on a magnet between each wash, and the supernatant was removed. Elution Buffer was added for releasing the antibody–antigen complex from the magnetic beads. The supernatant containing the antibody–antigen complex was then used to perform western blot analysis for detecting the ubiquitinated MYC protein.

Statistical analysis. One-way analysis of variance (ANOVA) following by Bonferroni's multiple comparison test was performed to conduct statistical analysis using GraphPad Prism 7.0 software (GraphPad Software, San Diego, CA, USA). Data are expressed as the mean±standard deviation (SD), and values of $p<0.05$ were indicative of significant differences.

Results

Cytotoxicity of gigantol. In order to further determine the effects of gigantol on cell proliferation, we first characterized the cell viability in response to gigantol treatment. Lung cancer cells were used to evaluate gigantol toxicity. The results showed that gigantol caused significant toxic effects on H460, A549, and H292 cells at concentrations of 50-200 μM in a dose-dependent manner (Figure 2A). Overall, gigantol treatment at concentrations lower than 20 μM caused no significant reduction in terms of cell viability in any of the tested cell lines (Figure 2A). Therefore, gigantol was used at 5-20 μM for further experiments.

Antiproliferative effect of gigantol. Gigantol at 5-20 μM was further investigated for the antiproliferative activity. The cells were cultured in growth medium in the presence or absence of gigantol for 1-3 days. The proliferation assay revealed that gigantol at 20 μM significantly reduced proliferation after 1 day of cultivation in H460 and A549 cells, however, gigantol at lower concentrations (5-10 μM) significantly suppressed

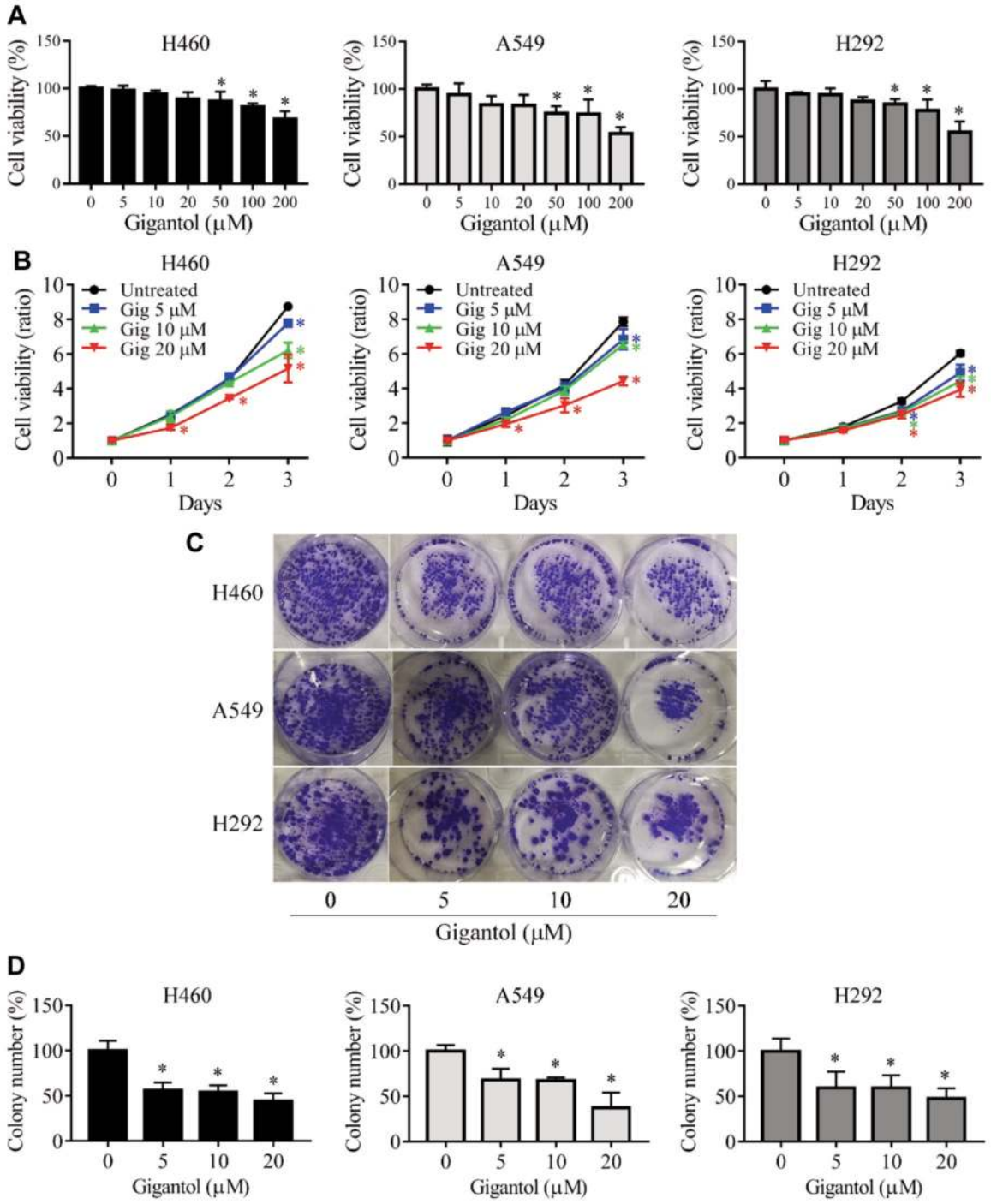

Figure 2. *A: Cytotoxicity of gigatol (Gig) was evaluated. Lung cancer cells were treated with 0-200 μM gigantol for 24 h. Cell viability was determined by an 3-(4,5-dimethylthiazol-2-yl)-2,5-diphenyltetrazolium bromide (MTT) assay. Cytotoxic effect of gigantol on H460, A549, and H292 was measured as a reduction of cell viability relative to that of untreated cells (100%) (n=5, *p<0.05, compared with the untreated cells). B: Antiproliferative effect of gigantol was evaluated. Lung cancer cells were treated with 0-20 μM gigantol for 3 days and the MTT assay was performed every 24 h. Cell viability at days 1-3 was compared to the viability at day 0 within each group, and data were plotted as a growth rate of each treatment group (The cell viability at day 0 was counted as 1). Relative growth of the gigantol-treated cells was compared with control cells for the same time of gigantol exposure (n=4, *p<0.05 compared with untreated cells at each time point). C: Colony-formation assay was performed to confirmed the antiproliferative effect of gigantol. Lung cancer cells were treated with 0-20 μM gigantol for 10 days and then were stained with crystal violet. Colonies with ≥50 cells were counted. Results showed the reduction of colony numbers of gigantol-treated cells in all tested cell lines. D: The percentage of colonies was calculated relative to that for untreated cells (n=3, *p<0.05 compared with the untreated cells). All data represent the mean±SD.*

proliferation at day 3. In H292 cells, gigantol at 5-20 μM showed an antiproliferative effect after 2 days of treatment (Figure 2B). Moreover, the antiproliferative activity of gigantol was confirmed using colony-formation assay of all tested cell lines as described in the Materials and Methods. The average colony number of the untreated control group was designated as 100% and the colony numbers of the gigantol-treated groups were calculated as a relative percentage. Gigantol at 5-20 μM significantly suppressed lung cancer cell growth in a dose-dependent manner (Figure 2C and D). Results from these two assays demonstrated that gigantol had an antiproliferative effect against lung cancer cells. As gigantol at 20 μM showed the strongest antiproliferative effect in both assays, this concentration was used for the proteomics analysis.

Quantitative proteomic analysis revealed the change of proliferation regulatory proteins in response to gigantol treatment. Having shown that gigantol negatively regulates proliferation of lung cancer cells, we next aimed to identify the key underlying mechanisms using proteomic analysis. The cells were treated with 20 μM gigantol or left untreated as control for 24 h, and then subjected to proteomic LC-MS/MS. The proteomic profiles of the two groups were obtained and bioinformatics analysis was performed. The analysis process is demonstrated as a flowchart in Figure 3A. The analysis identified 1, 767 proteins that were up-regulated and 2, 373 proteins that were down-regulated in gigantol-treated *versus* control cells. After deleting proteins whose gene names could not be identified by Uniprot database (accessed on 27 April 2020), the remaining 1, 763 up-regulated and 2, 368 down-regulated proteins were analyzed by the enrichment analysis tool, Enrichr (conducted on 27 April 2020). The GO annotations based on GO Consortium database were investigated and it was found that the GO term "regulation of cell proliferation (GO:0042127)" was the meaningful GO annotation associated with regulatory signaling of cell proliferation. Gigantol altered the expression of 156 proteins involved in the regulation of cell proliferation, of which 96 were down-regulated and 60 up-regulated. Subsequently, the hub proteins were clarified.

Gigantol targets MYC in lung cancer cells. To determine the most important hub protein that controlled cell proliferation, the differentially expressed proteins were subjected to PPI networks functional enrichment analysis using STRING (Figure 3B; conducted on 27 April, 2020), and the number of PPIs was analyzed using the function 'network analyzer' of Cytoscape software. The top 20 proteins that had the highest interactions with other proteins in the network were found to be AKT1, MYC, fibronectin (FN1), epidermal growth factor (EGF), KRAS, Janus kinase 2 (JAK2), KIT, breast cancer type 1 susceptibility protein (BRCA1), histone deacetylase 1 (HDAC1), insulinlike growth factor 1 receptor (IGF1R), Janus kinase 1 (JAK1), ABL1, cyclin dependent kinase 2 (CDK2), nitric oxide synthase 3 (NOS3), protein tyrosine kinase 2 (PTK2), histone deacetylase 2 (HDAC2), erb-b2 receptor tyrosine kinase 4 (ERBB4), bone morphogenetic protein 2 (BMP2), platelet-derived growth factor receptor A (PDGFRA), and insulin receptor (INSR) (Figure 3B). Their molecular functions were then determined from GO annotation using Panther software (conducted on 27 April 2020). Among these target candidates of gigantol, MYC had the most abundant PPIs in the network (>50 PPIs) and was down-regulated by gigantol (Figure 4A). It was also the only one that had transcription factor activity. This suggested that MYC was a key player in the mechanism of action of gigantol in suppression of cell proliferation. Therefore, we validated the effect of gigantol on MYC in H460, A549 and H292 lung cancer cells by western blot analysis.

The proteomic and protein interaction analysis pointed out that MYC was the dominant regulatory protein in cell proliferation in response to gigantol treatment. We then confirmed the validity of this in gigantol-treated cells. The cells were similarly treated with non-toxic concentrations of gigantol and the MYC level was determined by western blot analysis. Figure 4B shows that MYC expression was dramatically reduced in response to gigantol treatment. Gigantol at 10 and 20 μM significantly reduced the MYC level in all tested cells, while at 5 μM it significantly reduced the MYC level of H460 and A549 cells (Figure 4C). Overall, gigantol suppressed MYC expression in a dose-dependent manner. This result confirmed that gigantol down-regulates MYC protein in lung cancer cells.

Gigantol suppresses MYC through inhibition of GSK3β phosphorylation. Having shown that gigantol inhibited cell proliferation *via* MYC suppression, we next verified the underlying mechanisms of MYC protein level modulation. Figure 5A demonstrates a curated pathway of MYC regulation. Well-established evidence revealed that cellular MYC is regulated mainly *via* ubiquitin-proteasomal degradation and that phosphorylation at Thr58 by GSK3β was prerequisite for MYC ubiquitination. However, GSK3β function is regulated *via* phosphorylation at Ser9. Once GSK3β is phosphorylated and inactivated, MYC protein is more stable and the cellular MYC level is increased, resulting in cell proliferation (11). Therefore, the activation status of GSK3β was further investigated by western blot analysis. Cells were treated with gigantol at 0-20 μM for 24 hours and whole-cell lysates were harvested. The levels of phosphorylated and total forms of GSK3β were evaluated. Western blot results showed that gigantol at 5-20 μM significantly reduced the level of inactive GSK3β (phosphorylated GSK3β at Ser9), but rarely affected the total form of GSK3β in all tested cell liness (Figure 5B). The ratio of relative protein levels of phospho-GSK3β *versus* GSK3β was calculated to determine the level of GSK3β

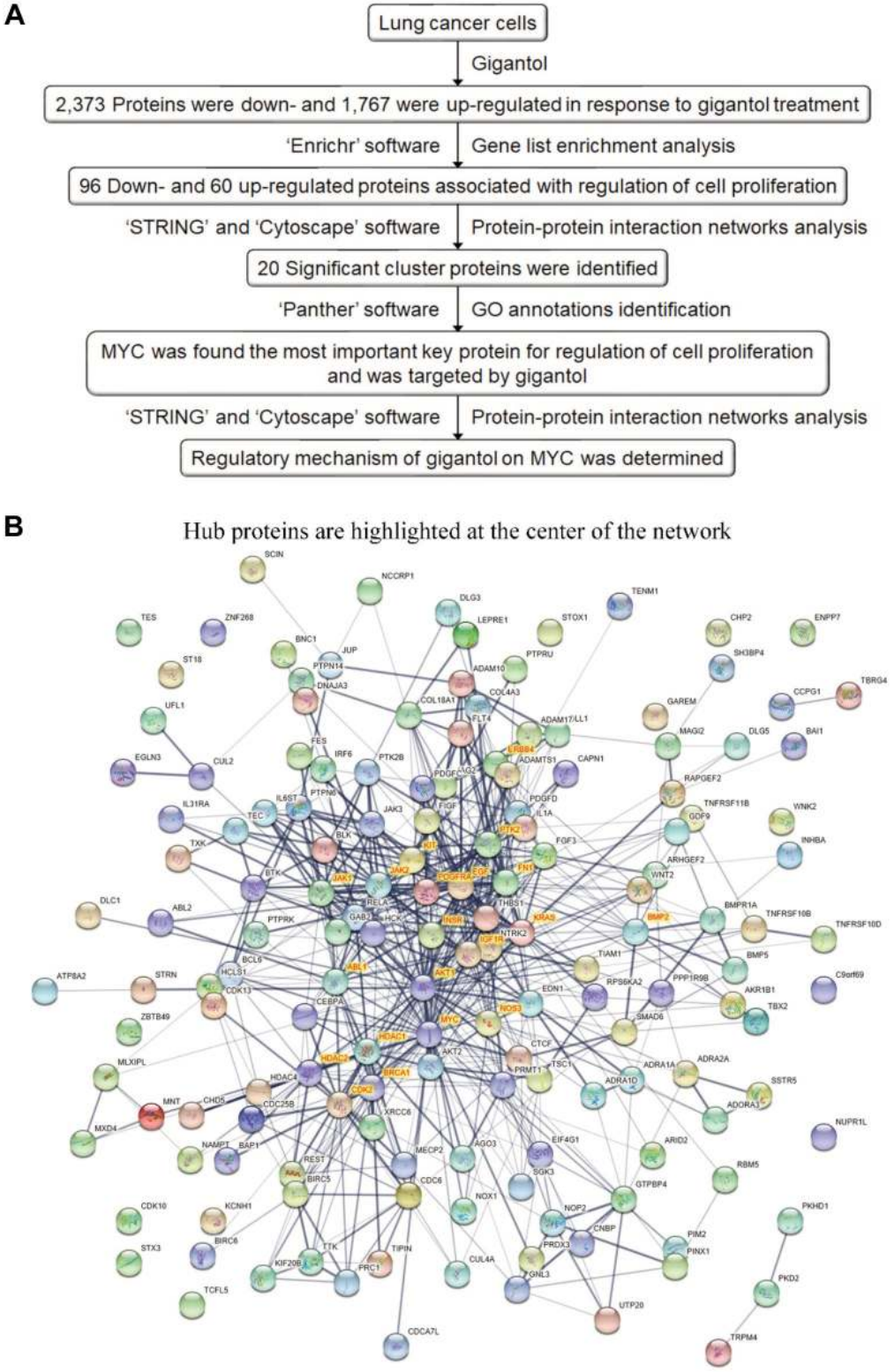

Figure 3. *A: Flowchart showing the bioinformatic analysis process of proteomic profiles obtained from untreated and gigantol-treated lung cancer cells. B: The protein–protein interaction (PPI) network of the differentially expressed proteins in gigantol-treated lung cancer cells, demonstrating the relationship between the 156 proteins associated with regulation of cell proliferation. Located in the center of the network, the proteins whose gene names are highlighted in yellow with red font were the top 20 proteins with the highest number of PPIs.*

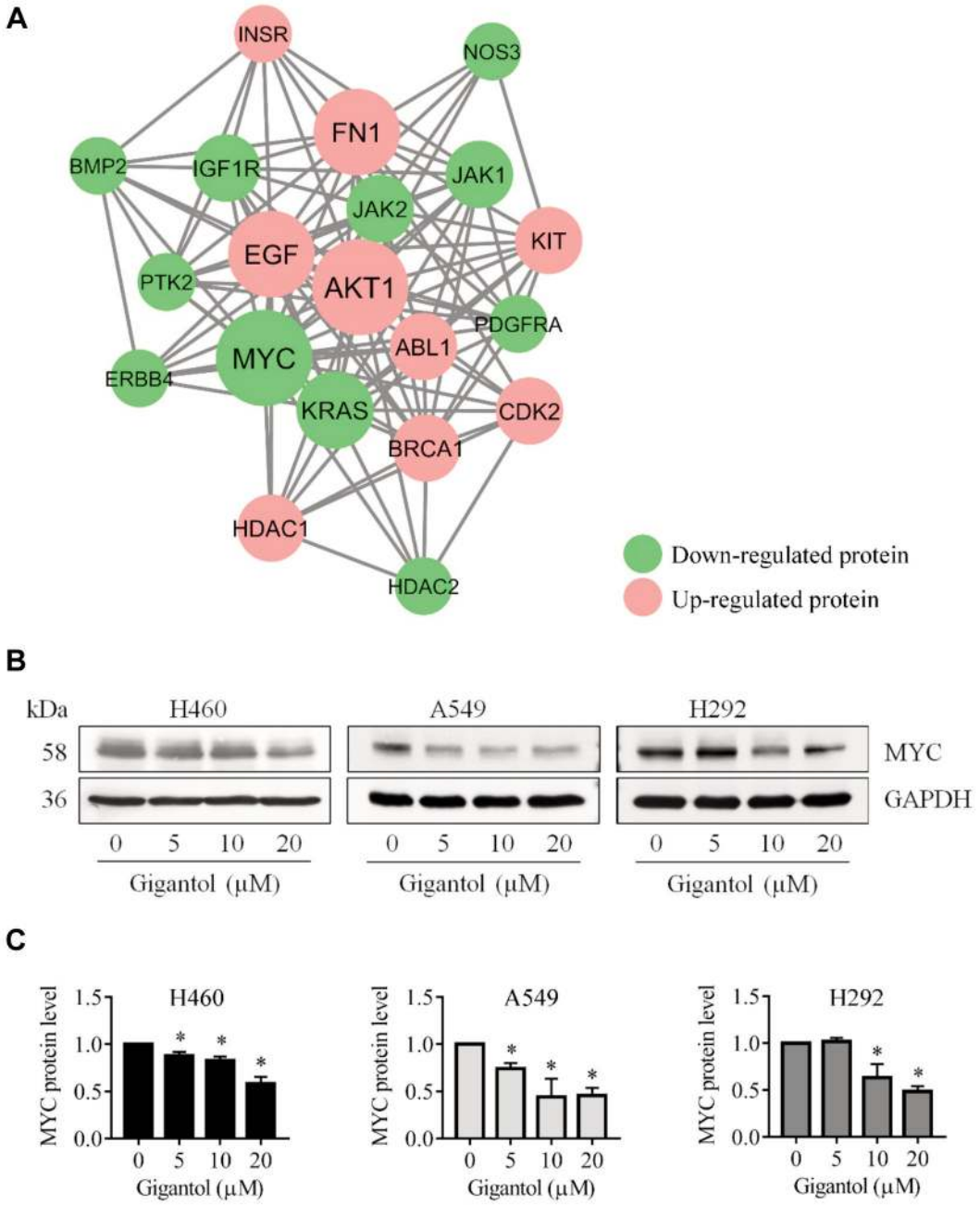

Figure 4. *A: Protein–protein interaction (PPI) network of 20 hub proteins demonstrating regulation status and significance level of the proteins affected by gigantol. The larger the node, the higher the number of PPIs. B: Lung cancer cells were treated with 0-20 μM gigantol for 24 h. Western blot analysis was performed to determine MYC level. Glyceraldehyde 3-phosphate dehydrogenase (GAPDH) was used to confirm equal loading of each protein sample. C: The band intensities of treatment groups were compared to the control group and are presented as fold-change. Data represent the mean±SD (n=3; *p<0.05 compared with the untreated control).*

inactivation (Figure 5C). The ratios indicated that GSK3β inactivation was significantly reduced by gigantol in a dose-dependent manner. This suggested that the increase of MYC degradation was triggered by a surge of active GSK3β.

Gigantol destabilizes MYC via ubiquitination-facilitated proteasomal degradation. Next, gigantol-induced MYC degradation was demonstrated using cycloheximide chasing assay. Gigantol at 20 μM was used in this assay as it reduced

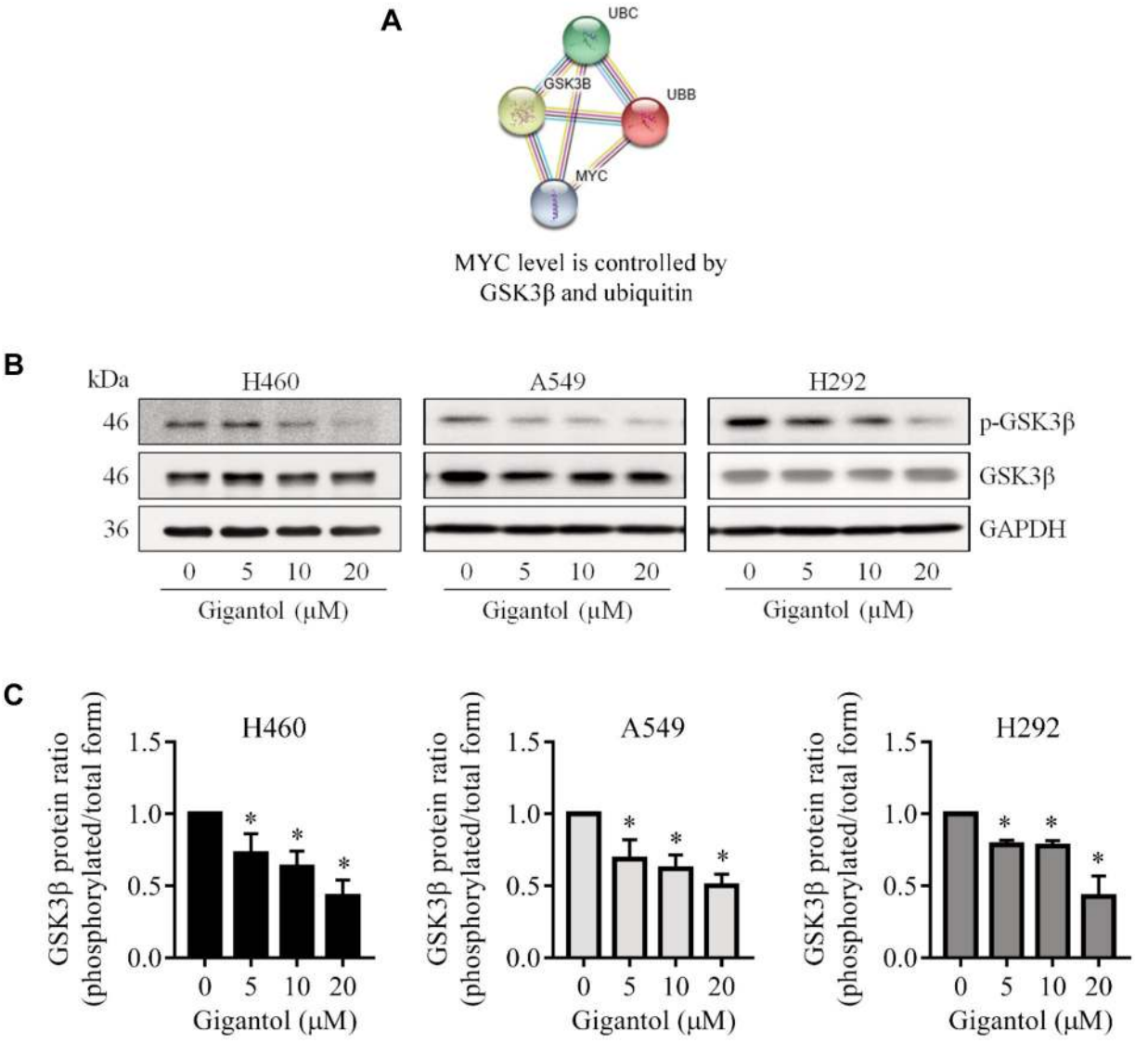

Figure 5. *A: Curated data showing the relationship between MYC, glycogen synthase kinase 3 beta (GSK3β), and ubiquitin. B: Western blot analysis was performed to determine the protein levels of phosphorylated and total forms of GSK3β with gigantol treatment. Glyceraldehyde 3-phosphate dehydrogenase (GAPDH) was used to confirm equal loading of each protein sample. C: The band intensities of treatment groups were compared to the control group and are presented as fold-change. Data represent the mean±SD (n=3; *p<0.05 compared with the untreated control).*

the MYC protein level more compared to 5 and 10 μM. Western blot analysis showed that gigantol significantly reduced the MYC protein level at after 15, 30, 45, and 60 min of treatment compared to the untreated control at the same time points in all tested cell lines (Figure 6A and B). The MYC half-life was calculated from an equation obtained from a regression curve. The MYC half-lives of untreated H460, A549, and H292 cells were 44.30±7.58, 38.63±3.75, and 38.52±7.45 min, while the half-lives of gigantol-treated cells were 26.41±3.24, 26.55±2.69, and 26.73±3.06 min, respectively (Figure 6C). This indicated that gigantol reduced the half-life of MYC significantly.

To demonstrate that this reduce in MYC stability was through proteasomal degradation of the protein, we utilized MG132, a potent selective proteasome inhibitor. The lung cancer cells were pretreated with MG132 0-20 μM for 1 h and then were left untreated or treated with gigantol for 1 h. Treatment with MG132 at all concentrations drastically increased the MYC level, which confirmed that MYC protein was degraded mainly through the proteasomal degradation pathway (Figure 7A and B). Treatment of the lung cancer cells with gigantol for 1 hour significantly reduced the MYC level, while pretreatment with MG132 (5–

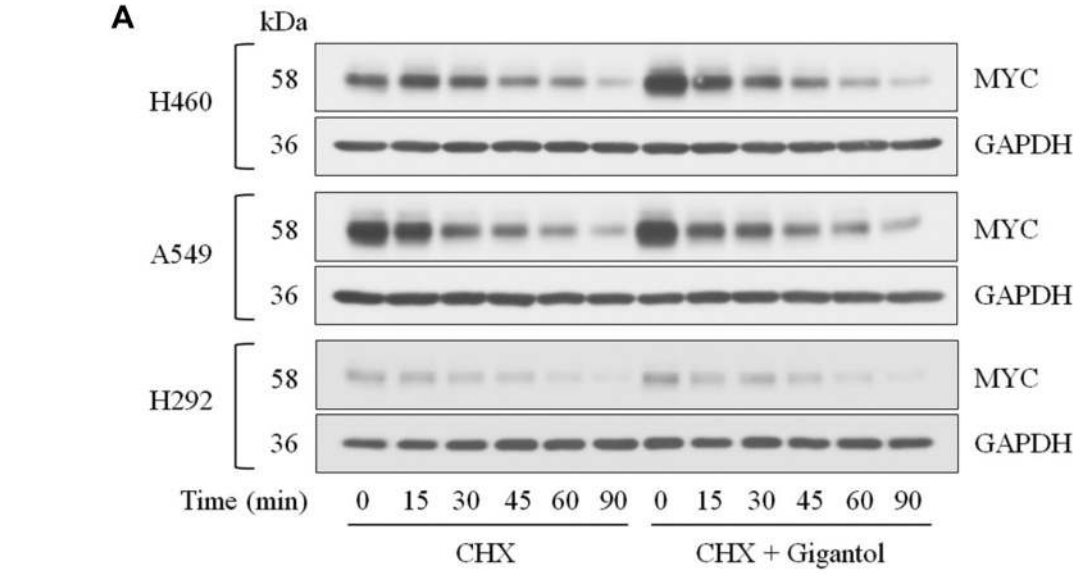

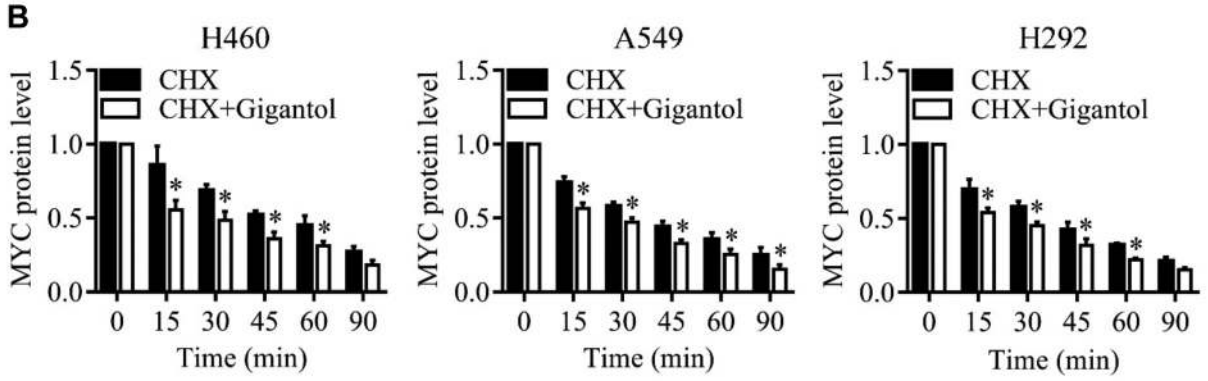

C

	MYC half-life (min)	
	Control	Gigantol
H460	44.30 ± 7.58	26.41 ± 3.24
A549	38.63 ± 3.75	26.55 ± 2.69
H292	38.52 ± 7.45	26.73 ± 3.06

Figure 6. *Cycloheximide (CHX) chasing assay was performed to measure MYC stability. Lung cancer cells were treated with 20 μM gigantol with or without 50 μg/ml CHX as indicated. A: Western blot analysis was performed for determined MYC levels. Glyceraldehyde 3-phosphate dehydrogenase (GAPDH) was used to confirm equal loading of each protein sample. B: The relative protein levels were calculated by densitometry (n=3, *p<0.05 compared with the untreated control at the same time). C: The half-life of MYC was calculated from the data.*

20 μM) reversed gigantol-induced MYC down-regulation (Figure 7A and B). Taken together, it could be concluded that gigantol induced MYC proteasomal degradation. The ubiquitination level of MYC was evaluated using immunoprecipitation and western blot analysis of the MYC–ubiquitin complex in the lung cancer cells treated with gigantol and in untreated control cells. After pretreating the cells with 10 μM MG132 for 1 h, the cells were left untreated or treated with 20 μM gigantol for another 1 h, then MYC complex was analyzed for conjugated ubiquitin through western blot analysis. Figure 7C and D show that gigantol treatment dramatically enhanced the formation of

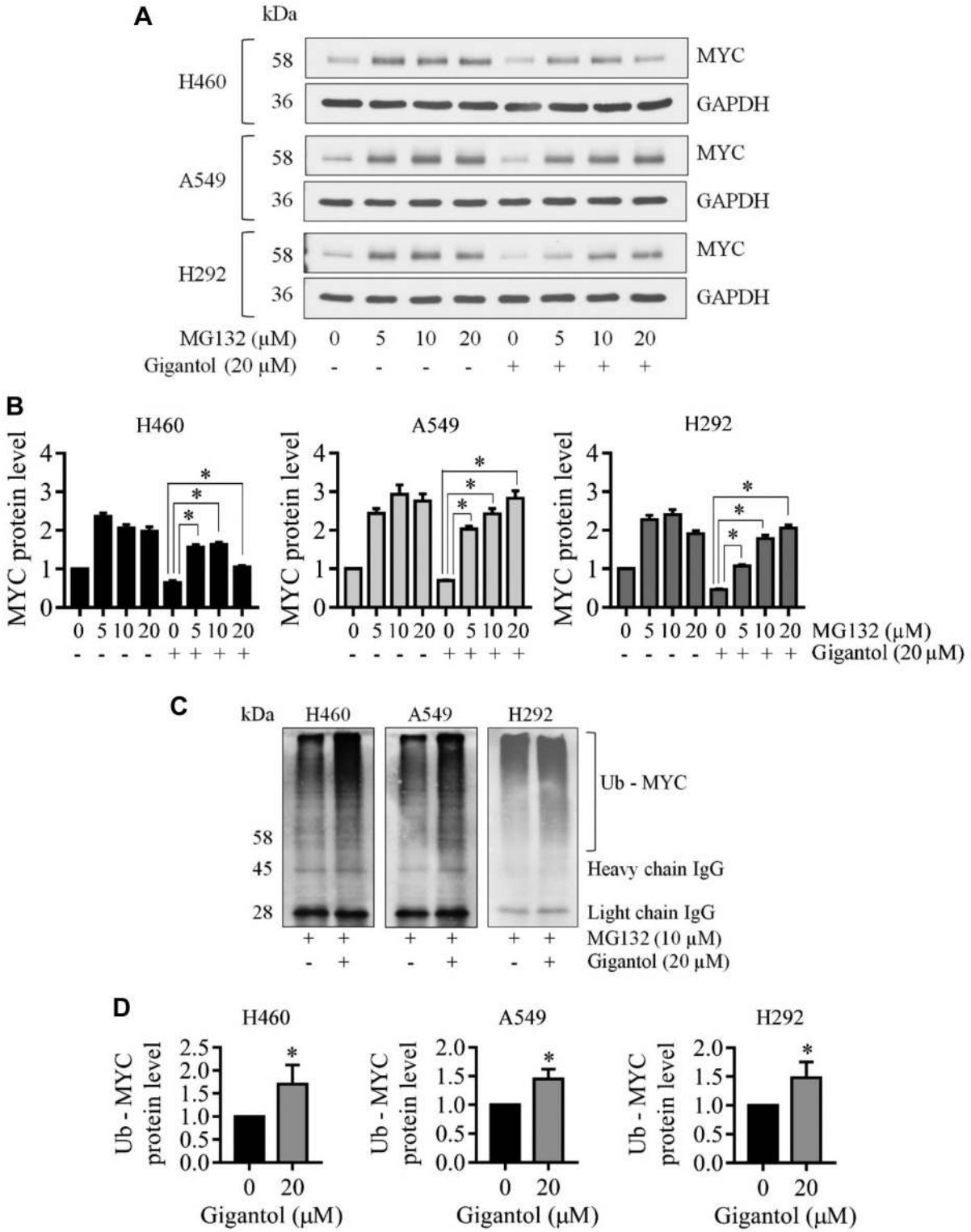

Figure 7. *A: Lung cancer cells were treated with a potent proteasome inhibitor, MG132 (0-20 μM) with or without gigantol (20 μM) for 1 h. MYC levels were measured using western blot analysis. Glyceraldehyde 3-phosphate dehydrogenase (GAPDH) was used to confirm equal loading of each protein sample. B: The band intensities were calculated by densitometry and compared to the untreated control cells (*p<0.05 compared with the non-MG132 gigantol-treated cells). C: Lung cancer cells were treated with MG132 (10 μM) with or without gigantol (20 μM) for 1 h. Protein lysates were then collected subsequent to MYC immunoprecipitation, and the ubiquitinated protein levels were measured by western blotting. D: Ubiquitinated MYC (Ub-MYC) levels were quantified using densitometry (*p<0.05 compared with the untreated control). All data represent the mean±SD (n=3).*

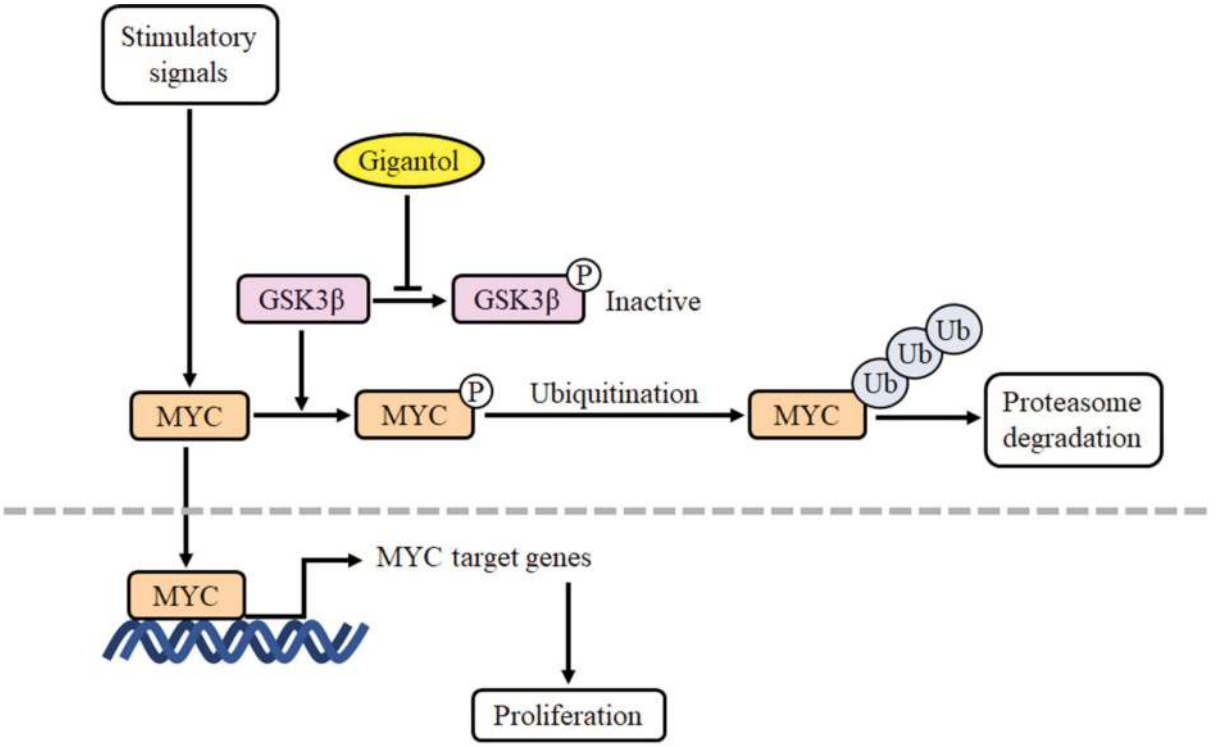

Figure 8. *A scheme presenting the mechanisms of action of gigantol in MYC-dependent cell growth suppression. Gigantol blocks phosphorylation of glycogen synthase kinase 3 beta (GSK3β), which subsequently enhances GSK3β-mediated MYC ubiquitin-proteasomal degradation.*

the MYC–ubiquitin complex compared to untreated controls of all tested cell lines. Taken together, the mechanism of action of gigantol was shown to be through the induction of MYC degradation *via* ubiquitin-proteasomal degradation.

Discussion

Gigantol has been reported to have anticancer properties against several cancer types including breast, liver, and lung cancer, while having a low toxic effect on normal cells (12, 15-17). Several effects of gigantol on aggressive phenotypes of lung cancer have been studied. Previous studies showed that gigantol suppressed EMT, migration and invasion, stem cell-like phenotype, and tumorigenicity (13, 14, 17). As far as we are aware, the antiproliferative effect of gigantol has not been explored. The present study is in line with above mentioned data and further supports the anticancer properties of gigantol in suppression of lung cancer cell growth. In order to evaluate cancer cell proliferation, the cytotoxicity of gigantol was a concerned as it might interfere in the result of the proliferation assay. Therefore, we first defined the concentrations of gigantol that caused no significant inhibitory effect on cancer cells within 24 h as a non-toxic concentration. The results showed that concentrations ≤20 μM had no toxic effect on lung cancer cells (Figure 2A), therefore this concentration was used for an antiproliferative evaluation. The proliferation assay demonstrated that gigantol reduced the growth rate of lung cancer cells and the colony formation assay showed that gigantol reduced the number of lung cancer cells with a colony-forming capacity in a dose-dependent manner (Figure 2B-D). Gigantol inhibited lung cancer cell proliferation effectively.

Cancer cell growth is a consequence of the activation of oncoproteins as well as dysregulation of proliferative proteins. Data from several studies revealed that certain oncoproteins such as MYC are overexpressed and activated in cancer (18-20). In general, MYC protein regulates biological functions, namely proliferation, apoptosis, and differentiation. It is called a master transcription factor since MYC participates in transcription of up to 15% of the entire genome (21). In cancer, overexpression of MYC is correlated with poor prognosis and unfavorable patient survival (22), and the transient silencing of MYC was shown to sufficiently inhibit cancer cell proliferation (8). These data have highlighted the fact that MYC is a critical protein for enhancing cancer cell growth and inhibition of such a protein may offer an effective strategy for management of the disease. Here we demonstrated that MYC was a key protein affected by the treatment of gigantol using proteomics and bioinformatics approaches (Figure 3A). Based on the

enrichment analysis results, "regulation of cell proliferation" in GO biological processes was the nearest term related to cell proliferation. We defined hub proteins because such proteins would affect several effectors or signaling pathways and have a major impact on cellular processes overall. Changes of hub proteins by treatment would effect cancer cell proliferation. We defined the top 20 hub proteins as potential candidate target of gigantol (Figure 3B). Since the proliferation assay and colony-formation assay indicated that gigantol inhibited cancer cell growth, the target in response to gigantol treatment should be proteins that facilitate cell proliferation and which were down-regulated by gigantol, or up-regulated proteins which inhibit cell proliferation. It appeared that MYC, which is a pro-proliferative protein, was down-regulated by gigantol with the most abundant PPIs (Figure 4A). Furthermore, MYC is a transcription factor whose function correlated with its expression level. Thus, a small change in MYC protein level might have a large effect on cell division processes. MYC is a well-known proto-oncogene which controls several proteins involved in the cell cycle and is crucial for cancer cell growth (6). Moreover, phosphoinositide 3-kinase (PI3K)/AKT, mitogen-activated protein kinase (MAPK), and JAK/signal transducer and activator of transcription 3 (STAT) pathways induce cancer proliferation through MYC regulation (23-25). Therefore, we considered MYC as a target of gigantol-mediated inhibition of proliferation. The MYC expression level was validated in lung cancer cells, and western blot analysis demonstrated that MYC levels in gigantol treated cells was significantly reduced (Figure 4B and C). The protein analysis confirmed that gigantol reduced the cellular MYC level in lung cancer cells.

We also investigated the mechanisms that caused attenuation of the MYC level. It is known that GSK3β promotes proteasomal degradation of MYC by phosphorylating MYC at Thr58 and enhancing MYC degradation *via* the ubiquitin-proteasome pathway. MYC is also positively regulated by AKT *via* AKT-mediated GSK3β inactivation (11). Previous studies demonstrated that gigantol inhibited AKT function by reducing an active form of AKT (phosphorylated AKT at Ser473) in lung cancer (14, 17), therefore it was possible that gigantol might enhance GSK3β function. Nevertheless, an effect of gigantol on GSK3β was unclear. We tested this hypothesis by western blot analysis. The results indicated that gigantol treatment reduced the level of Ser9 p-GSK3β (the inactive form) but not total GSK3β (Figure 5B and C). This suggests that gigantol attenuates GSK3β inactivation, which leads to an increase in the active form of GSK3β and accelerates MYC degradation, as demonstrated by the reduction of MYC half-life in the cycloheximide chasing assay (Figure 6). We performed inhibition of proteasomal degradation using MG132 and the results confirmed that MYC was indeed degraded mainly through the proteasome pathway. MG132-treated cells had a higher MYC level because MYC degradation was blocked and MYC accumulated in the cells (Figure 7A and B). Moreover, MG132 was able to reverse an inhibitory effect of gigantol on MYC level (Figure 7A and B), which confirmed that gigantol destabilized MYC through proteasomal degradation. Next, we verified the level of ubiquitin-MYC conjugation for ubiquitination was required for the recognition of the proteasome. Immunoprecipitation followed by western blot analysis was performed and the results indicated that MYC ubiquitination was significantly increased in gigantol-treated cells (Figure 7C and D). These data show that MYC degradation was increased by gigantol since ubiquitination was the critical process for prompting ubiquitin-proteasomal degradation.

MYC is a potential target for cancer treatment as it plays prominent roles in tumorigenesis and cancer progression. Various strategies for modulating MYC expression have been suggested, such as targeting the up-stream signaling pathways which destabilize MYC protein [reviewed in (6)]. Natural flavonoids that modulated MYC were intensively explored. For example, taxifolin, a natural plant flavonoid found in the barks of *Cedrus brevifolia*, *Cedrus brevifolia* (Hooker fil.), *Laric siberica* (ledeb.) and *Texus chinensis*, was demonstrated to inhibit osteosarcoma cell proliferation and suppress tumor growth in nude mice xenograft model through AKT/MYC inhibition (26). In line with the above context, the present study provides a detail of a key molecular mechanism by which gigantol suppresses MYC and supports its potential use and development for cancer treatment (Figure 8).

The present study provided molecular mechanisms for the effects of gigantol on cell proliferation of lung cancer cells using proteomic and bioinformatic analysis. Gigantol inhibited lung cancer proliferation by the reduction of MYC stabilization through enhancing GSK3β-mediated ubiquitin-proteasomal degradation. This finding on the mechanism of regulation of cell proliferation by gigantol may have vital implications in lung cancer management.

Conflicts of Interest

The Authors declare no conflicts of interest.

Authors' Contributions

Nattanan Losuwannarak: Methodology, formal analysis, writing - original draft. Sittirak Roytrakul: Formal analysis, resources. Pithi Chanvorachote: Conceptualization, supervision, data curation, resources, writing - review and editing.

Acknowledgements

The Authors would like to acknowledge the Pharmaceutical Research Instrument Center, Faculty of Pharmaceutical Sciences, Chulalongkorn University for providing equipment.

This research was supported by the 90th Anniversary of Chulalongkorn University, Rachadapisek Sompote Fund. The funding source had no involvement in study design, in the collection, analysis and interpretation of data, in the writing of the report, and in the decision to submit the article for publication.

References

1 Hanahan D and Weinberg RA: Hallmarks of cancer: The next generation. Cell *144(5)*: 646-674, 2011. PMID: 21376230. DOI: 10.1016/j.cell.2011.02.013

2 van Diest PJ, van der Wall E and Baak JP: Prognostic value of proliferation in invasive breast cancer: A review. J Clin Pathol *57(7)*: 675-681, 2004. PMID: 15220356. DOI: 10.1136/jcp.2003.010777

3 Miura K, Hamanaka K, Koizumi T, Kawakami S, Kobayashi N and Ito KI: Solid component tumor doubling time is a prognostic factor in non-small cell lung cancer patients. J Cardiothorac Surg *14(1)*: 57, 2019. PMID: 30871590. DOI: 10.1186/s13019-019-0879-x

4 Eymin B and Gazzeri S: Role of cell cycle regulators in lung carcinogenesis. Cell Adh Migr *4(1)*: 114-123, 2010. PMID: 20139697. DOI: 10.4161/cam.4.1.10977

5 Yuan M, Huang L-L, Chen J-H, Wu J and Xu Q: The emerging treatment landscape of targeted therapy in non-small-cell lung cancer. Signal Transduct Target Ther *4(1)*: 61, 2019. PMID: 31871778. DOI: 10.1038/s41392-019-0099-9

6 Chen H, Liu H and Qing G: Targeting oncogenic MYC as a strategy for cancer treatment. Signal Transduct Target Ther *3:* 5, 2018. PMID: 29527331. DOI: 10.1038/s41392-018-0008-7

7 Lim DY, Shin SH, Lee M-H, Malakhova M, Kurinov I, Wu Q, Xu J, Jiang Y, Dong Z, Liu K, Lee KY, Bae KB, Choi BY, Deng Y, Bode A and Dong Z: A natural small molecule, catechol, induces MYC degradation by directly targeting ERK2 in lung cancer. Oncotarget *7(23)*: 35001-35014, 2016. PMID: 27167001. DOI: 10.18632/oncotarget.9223

8 Liu X, Wu C, Wu Y, Tang Y and Du J: MYC silencing impedes cell proliferation and enhances cytotoxicity of cisplatin in non-small cell lung cancer. Int J Clin Exp Pathol *9(9)*: 9199-9205, 2016. Available at http://www.ijcep.com/files/ijcep0028820.pdf [Last accessed on September 1st, 2020]

9 Evangelisti C, Chiarini F, Paganelli F, Marmiroli S and Martelli AM: Crosstalks of GSK3 signaling with the mTOR network and effects on targeted therapy of cancer. Biochim Biophys Acta Mol Cell Res *1867(4)*: 118635, 2020. PMID: 31884070. DOI: 10.1016/j.bbamcr.2019.118635

10 Zheng H, Saito H, Masuda S, Yang X and Takano Y: Phosphorylated GSK3β-ser9 and EGFR are good prognostic factors for lung carcinomas. Anticancer Res 27*(5B)*: 3561-3569, 2007. PMID: 17972518.

11 Sears RC: The life cycle of MYC: From synthesis to degradation. Cell Cycle *3(9)*: 1131-1135, 2004. PMID: 15467447. DOI: 10.4161/cc.3.9.1145

12 Charoenrungruang S, Chanvorachote P, Sritularak B and Pongrakananon V: Gigantol-induced apoptosis in lung cancer cell through mitochondrial-dependent pathway. Thai J Pharm Sci *38:* 67-73, 2014.

13 Unahabhokha T, Chanvorachote P, Sritularak B, Kitsongsermthon J and Pongrakhananon V: Gigantol inhibits epithelial to mesenchymal process in human lung cancer cells. Evid Based Complement Alternat Med *2016:* 4561674, 2016. PMID: 27651818. DOI: 10.1155/2016/4561674

14 Bhummaphan N and Chanvorachote P: Gigantol suppresses cancer stem cell-like phenotypes in lung cancer cells. Evid Based Complement Alternat Med *2015:* 836564, 2015. PMID: 27651818. DOI: 10.1155/2016/4561674

15 Yu S, Wang Z, Su Z, Song J, Zhou L, Sun Q, Liu S, Li S, Li Y, Wang M, Zhang GQ, Zhang X, Liu ZJ and Lu D: Gigantol inhibits WNT/beta-catenin signaling and exhibits anticancer activity in breast cancer cells. BMC Complement Altern Med *18(1)*: 59, 2018. PMID: 29444668. DOI: 10.1186/s12906-018-2108-x

16 Chen H, Huang Y, Huang J, Lin L and Wei G: Gigantol attenuates the proliferation of human liver cancer HepG2 cells through the PI3K/AKT/NF-kappaB signaling pathway. Oncol Rep *37(2)*: 865-870, 2017. PMID: 27959444. DOI: 10.3892/or.2016.5299

17 Losuwannarak N, Maiuthed A, Kitkumthorn N, Leelahavanichkul A, Roytrakul S and Chanvorachote P: Gigantol targets cancer stem cells and destabilizes tumors *via* the suppression of the PI3K/AKT and JAK/STAT pathways in ectopic lung cancer xenografts. Cancers *11(12)*, 2032, 2019. PMID: 31861050. DOI: 10.3390/cancers11122032

18 Chanvorachote P, Sriratanasak N and Nonpanya N: c-MYC contributes to malignancy of lung cancer: A potential anticancer drug target. Anticancer Res *40(2)*: 609-618, 2020. PMID: 32014901. DOI: 10.21873/anticanres.13990

19 Xu J, Chen Y and Olopade OI: MYC and breast cancer. Genes Cancer *1(6)*: 629-640, 2010. PMID: 21779462. DOI: 10.1177/1947601910378691

20 Koh CM, Bieberich CJ, Dang CV, Nelson WG, Yegnasubramanian S and De Marzo AM: MYC and prostate cancer. Genes Cancer *1(6)*: 617-628, 2010. PMID: 21779461. DOI: 10.1177/1947601910379132

21 Dang CV, O'Donnell KA, Zeller KI, Nguyen T, Osthus RC and Li F: The MYC target gene network. Semin Cancer Biol *16(4)*: 253-264, 2006. PMID: 16904903. DOI: 10.1016/j.semcancer.2006.07.014

22 Seo AN, Yang JM, Kim H, Jheon S, Kim K, Lee CT, Jin Y, Yun S, Chung JH and Paik JH: Clinicopathologic and prognostic significance of *c-MYC* copy number gain in lung adenocarcinomas. Br J Cancer *110(11)*: 2688-2699, 2014. PMID: 24809777. DOI: 10.1038/bjc.2014.218

23 Buckler JL, Liu X and Turka LA: Regulation of T-cell responses by PTEN. Immunol Rev *224:* 239-248, 2008. PMID: 18759931. DOI: 10.1111/j.1600-065X.2008.00650.x

24 Wang Q, Tan R, Zhu X, Zhang Y, Tan Z, Su B and Li Y: Oncogenic K-RAS confers SAHA resistance by up-regulating *HDAC6* and c-MYC expression. Oncotarget *7(9)*: 10064-10072, 2016. PMID: 26848526. DOI: 10.18632/oncotarget.7134

25 Choi JW, Schroeder MA, Sarkaria JN and Bram RJ: Cyclophilin B supports MYC and mutant P53-dependent survival of glioblastoma multiforme cells. Cancer Res *74(2)*: 484-496, 2014. PMID: 24272483. DOI: 10.1158/0008-5472.CAN-13-0771

26 Chen X, Gu N, Xue C and Li B: Plant flavonoid taxifolin inhibits the growth, migration and invasion of human osteosarcoma cells. Mol Med Rep *17:* 3239-3245, 2018. PMID: 29257319. DOI: 10.3892/mmr.2017.8271

Received August 4, 2020
Revised August 31, 2020
Accepted September 1, 2020